N-Glycan structures and N-glycosylation sites of mouse soluble intercellular adhesion molecule-1 revealed by MALDI-TOF and FTICR mass spectrometry

Author(s):
Otto, Vivianne I.; Damoc, Eugen; Cueni, Leah N.; Schürpf, Thomas; Frei, Renate; Ali, Sarah; Callewaert, Nico; Moise, Adrian; Leary, Julie A.; Folkers, Gerd; Przybylski, Michael

Publication date:
2006-11

Permanent link:
https://doi.org/10.3929/ethz-b-000035936

Originally published in:
Glycobiology 16(11), https://doi.org/10.1093/glycob/cwl032

Glycobiology vol. 16 no. 11 pp. 1033–1044, 2006
doi:10.1093/glycob/cwl032
Advance Access publication on July 28, 2006

N-Glycan structures and N-glycosylation sites of mouse soluble intercellular adhesion molecule-1 revealed by MALDI-TOF and FTICR mass spectrometry

Vivianne I. Otto[1,2], Eugen Damoc[4,5], Leah N. Cueni[2], Thomas Schürpf[2], Renate Frei[2], Sarah Ali[2], Nico Callewaert[3], Adrian Moise[4], Julie A. Leary[5], Gerd Folkers[2], and Michael Przybylski[4]

[2]Institute of Pharmaceutical Sciences, Department of Chemistry and Applied Biosciences; [3]GlycoINIT and Institute of Microbiology, Department of Biology, ETH Zurich, Switzerland; [4]Department of Chemistry, Laboratory of Analytical Chemistry, University of Konstanz, 78457 Konstanz, Germany; and [5]Genome Center, UC Davis, Davis, CA 95616

Received on January 2, 2006; revised on July 26, 2006; accepted on July 26, 2006

Intercellular adhesion molecule-1 (ICAM-1) is a heavily N-glycosylated transmembrane protein comprising five extracellular Ig-like domains. The soluble isoform of ICAM-1 (sICAM-1), consisting of its extracellular part, is elevated in the cerebrospinal fluid of patients with severe brain trauma. In mouse astrocytes, recombinant mouse sICAM-1 induces the production of the CXC chemokine macrophage inflammatory protein-2 (MIP-2). MIP-2 induction is glycosylation dependent, as it is strongly enhanced when sICAM-1 carries sialylated, complex-type *N*-glycans as synthesized by wild-type Chinese hamster ovary (CHO) cells. The present study was aimed at elucidating the N-glycosylation of mouse sICAM-1 expressed in wild-type CHO cells with regard to sialylation, *N*-glycan profile, and N-glycosylation sites. Ion-exchange chromatography and matrix-assisted laser desorption ionization time-of-flight (MALDI-TOF) mass spectrometry (MS) of the released *N*-glycans showed that sICAM-1 mostly carried di- and trisialylated complex-type *N*-glycans with or without one fucose. In some sialylated *N*-glycans, one *N*-acetylneuraminic acid was replaced by *N*-glycolylneuraminic acid, and ~4% carried a higher number of sialic acid residues than of antennae. The N-glycosylation sites of mouse sICAM-1 were analyzed by MALDI-Fourier transform ion cyclotron resonance (FTICR)-MS and nanoLC-ESI-FTICR-MS of tryptic digests of mouse sICAM-1 expressed in the Lec1 mutant of CHO cells. All nine consensus sequences for N-glycosylation were found to be glycosylated. These results show that the *N*-glycans that enhance the MIP-2-inducing activity of mouse sICAM-1 are mostly di- and trisialylated complex-type *N*-glycans including a small fraction carrying more sialic acid residues than antennae and that the nine N-glycosylation sites of mouse sICAM-1 are all glycosylated.

[1]To whom correspondence should be addressed; e-mail: vivianne.otto@pharma.ethz.ch

Key words: Fourier transform ion cyclotron resonance mass spectrometry/glycosylation–function relationships/ N-glycosylation/oligosialic acid/mouse soluble intercellular adhesion molecule-1

Introduction

Intercellular adhesion molecule-1 (ICAM-1) is a heavily N-glycosylated type I transmembrane protein belonging to the Ig superfamily of adhesion molecules. It consists of five extracellular Ig-like domains, a single transmembrane segment, and a short intracellular domain. ICAM-1 also occurs as a soluble glycoprotein consisting of the extracellular part of membrane-bound ICAM-1. Soluble ICAM-1 (sICAM-1) may derive from either alternative RNA splicing or proteolytic cleavage of membrane-bound ICAM-1 (King *et al*., 1995; Budnik *et al*., 1996; Lyons and Benveniste, 1998). ICAM-1 is normally expressed at low levels on vascular endothelium, lymphocytes, and macrophages. In response to inflammatory stimuli and injury, ICAM-1 expression is enhanced and can also be induced on many other cell types (Dustin *et al*., 1986; Sobel *et al*., 1990). After severe brain trauma, the number of ICAM-1-positive brain vessels and the concentration of sICAM-1 in cerebrospinal fluid are strongly increased (Otto *et al*., 2000; Rancan *et al*., 2001).

The biological role of membrane-bound ICAM-1 in leukocyte extravasation has been studied extensively. ICAM-1 on the surface of vascular endothelial cells mediates the firm adhesion and transendothelial migration of activated leukocytes by binding to the β2 integrins leukocyte function-associated antigen-1 (LFA-1) and macrophage antigen-1 (Mac-1) (Marlin and Springer, 1987; Diamond *et al*., 1990). The binding sites for LFA-1 and Mac-1 are located on the first and third N-terminal Ig domain of ICAM-1, respectively (Diamond *et al*., 1991). Beyond its ability to provide the adhesion sites for leukocytes, membrane-bound ICAM-1 behaves as a signal transducer, allowing brain endothelial cells and astrocytes to respond actively to leukocyte adhesion (Greenwood *et al*., 2002; Millan and Ridley, 2005). The functions of sICAM-1 are less well understood. Some studies suggest that sICAM-1 may have anti-inflammatory properties, as human sICAM-1 expressed in baby hamster kidney (BHK) and Chinese hamster ovary (CHO) cells and mouse sICAM-1 expressed in Sf9 insect cells acted as competitive inhibitors of leukocyte adhesion to vascular endothelium (Meyer *et al*., 1995; Rieckmann *et al*., 1995; Kusterer *et al*., 1998). Other studies suggest that sICAM-1 has pro-inflammatory signaling functions. In this regard, recombinant human sICAM-1

expressed in CHO cells was shown to enhance lymphocyte proliferation and cytokine production during the mixed lymphocyte response (McCabe *et al.*, 1993). Furthermore, sICAM-1 seems to be involved in neuroinflammation. sICAM-1 levels are elevated in the cerebrospinal fluid of patients with severe brain trauma, and recombinant mouse sICAM-1 expressed in mouse fibroblasts induces the production of the CXC chemokine macrophage inflammatory protein-2 (MIP-2) in cultured mouse astrocytes (Otto *et al.*, 2000, 2002). Although the signaling function of human sICAM-1 in lymphocytes is mediated through its binding to LFA-1, MIP-2 induction in mouse astrocytes is mediated by an as yet undefined receptor.

The various functions of ICAM-1 and sICAM-1 appear to be differentially regulated by glycosylation. An early study reported that binding of human ICAM-1 present on transfected L-cells to immobilized LFA-1 was not influenced by glycosylation (Diamond *et al.*, 1991). The binding of human ICAM-1 to Mac-1 was however found to be hindered if sialylated or desialylated complex-type *N*-glycans were present on the third Ig domain of ICAM-1 (Figure 1; Diamond *et al.*, 1991). In contrast, one study dealing with mouse sICAM-1 showed that sialylated and galactosylated complex-type *N*-glycans strongly enhanced the ability of recombinant mouse sICAM-1 expressed in wild-type CHO cells to induce MIP-2 production in astrocytes (Otto *et al.*, 2004). It seems therefore that binding to different binding partners or receptors of ICAM-1/sICAM-1 is differentially regulated by glycosylation.

The mechanisms by which the glycosylation of a protein may influence its overall three-dimensional structure, favor or hinder its interactions with binding partners and/or its ability to induce cell signaling are poorly understood. To get a handle on these questions, the elucidation of the glycan structures on proteins with glycosylation-dependent functions and of the sites to which they are attached is of primary importance. The glycosylation and N-glycosylation sites of human ICAM-1 have been analyzed in a few previous studies. In human sICAM-1 expressed in CHO cells, all eight potential N-glycosylation sites were found to be glycosylated (Bloom *et al.*, 1996). They carried mostly sialylated, complex-type *N*-glycans with or without a fucose, but some hybrid-type *N*-glycans were present as well. In contrast, a study based on the crystal structure of Ig domains 3–5 of human ICAM-1 expressed in the Lec3.2.8.1 mutant of CHO cells suggested that one potential N-glycosylation site (N-379) was not glycosylated (Yang *et al.*, 2004). To date, the glycosylation of mouse ICAM-1 has not been analyzed in detail. Mouse ICAM-1 displays 55% amino acid sequence homology with human ICAM-1. Five consensus sequences for N-glycosylation are conserved in human and mouse ICAM-1 (N-156/158, N-175/177, N-240, N-358/361, N-379/382). All potential N-glycosylation sites of human ICAM-1 are located between Ig domain 2 and the interdomain interface following Ig domain 4 (Figure 1). In contrast, the mouse ICAM-1 sequence additionally comprises potential N-glycosylation sites in the first and fifth Ig domains (Figure 3A).

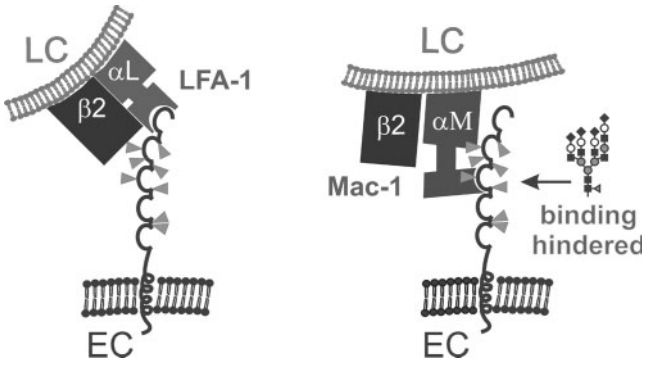

Fig. 1. Biological functions of human ICAM-1 and how they are influenced by glycosylation. The five open circles symbolize the five Ig domains of human ICAM-1 and the eight predicted N-glycosylation sites are pointed out by gray triangles. Binding of the first N-terminal Ig domain of human ICAM-1 on endothelial cells (ECs) to LFA-1 (heterodimer of the αL and β2 integrin subunits) on leukocytes (LCs) is not altered by glycosylation, whereas the presence of large complex-type *N*-glycans (symbolic representation of monosaccharides as in Figure 2B) on the third Ig domain hinders binding to Mac-1 (heterodimer of the αM and β2 integrin subunits) (Diamond *et al.*, 1991).

Owing to its functional importance in the regulation of astrocytic MIP-2 production, we aimed at elucidating the N-linked glycosylation of mouse sICAM-1 expressed in wild-type CHO cells with regard to the number of sialic acids, structures, and relative abundances of the sialylated *N*-glycans as well as the sites on the protein to which *N*-glycans are attached. Previously, we had analyzed the sialylation of sICAM-1 from wild-type CHO cells by isoelectric focusing (IEF) before and after treatment with neuraminidase (Otto *et al.*, 2004). Neuraminidase-treated sICAM-1 had an apparent isoelectric point (pI) of 5.9. However, untreated sICAM-1 displayed a pI of <3.6 and was therefore not visible on the IEF gels. To overcome the limitations of IEF, we chose an approach based on the enzymatic release of *N*-glycans, fluorescent labeling, and high-performance ion-exchange chromatography (HP-IEC) followed by matrix-assisted laser desorption ionization-time of flight (MALDI-TOF) mass spectrometry (MS). The sites on mouse sICAM-1 carrying *N*-glycans were determined by MALDI- and electrospray ionization (ESI)-Fourier transform ion cyclotron resonance mass spectrometry (FTICR-MS) of tryptic peptides obtained from mouse sICAM-1 expressed in the Lec1 mutant of CHO cells with or without prior endoglycosidase treatment. sICAM-1 expressed in Lec1 cells was used for this analyses, because its homogeneous glycosylation allows for unambiguous interpretation of MS results. Additionally, the knowledge of the N-glycosylation pathway allows to predict that the occupancy of N-glycosylation sites is the same in Lec1 and wild-type CHO cells.

Results

N-*Glycans present on mouse sICAM-1 from wild-type CHO cells*

To characterize the function-enhancing, sialylated *N*-glycans of mouse sICAM-1 expressed in wild-type CHO cells, we used an approach based on HP-IEC followed by MALDI-TOF-MS (Townsend *et al.*, 1996; Viseux *et al.*, 2001). *N*-Glycans were released from sICAM-1 by peptide *N*-glycosidase F

(PNGase F) treatment, labeled with fluorescent 2-aminobenzamide (2-AB) by reductive amination, and separated by HP-IEC. The peak fractions were collected and analyzed by MALDI-TOF-MS. To determine the composition and structures of the *N*-glycans, we compared the masses obtained by MALDI-TOF-MS with molecular masses calculated from N-linked oligosaccharide structures commonly found in CHO cells, and the identity and number of terminal negatively charged substituents of the more abundant components were confirmed by MALDI-TOF/TOF tandem MS.

HP-IEC separated the *N*-glycans released from sICAM-1 into 11 major peak fractions (Figure 2A), and

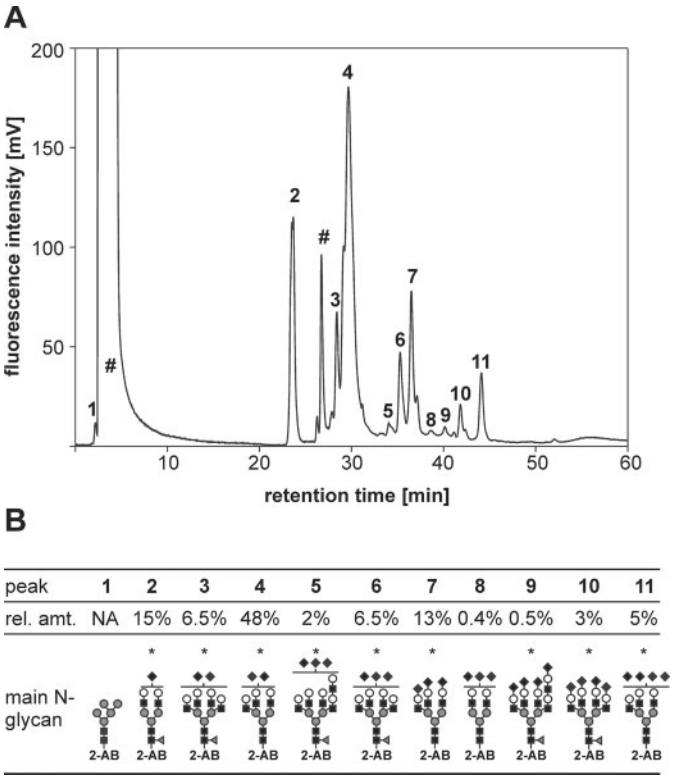

Fig. 2. *N*-Glycans present on mouse sICAM-1 from CHO cells. (**A**) The *N*-glycans of mouse soluble ICAM-1 from CHO cells were released by PNGase F treatment, purified over Carbograph, fluorescently labeled with 2-AB, and injected onto the GlycoSep C HP-IEC column, which had been equilibrated with 80% ACN. The ACN content was linearly decreased to 20% over 13 min and then maintained at this level. Between 13 and 48 min, a linear gradient of ammonium acetate pH 4.5 from 0 to 160 mM was run. The separation of fluorescent compounds was monitored by fluorescence detection. (**B**) The relative amounts (rel. amt.) of the total glycans contained in each peak of the chromatogram shown in A were calculated from the peak areas (mean from two independent analyses; the sum of the areas of the peaks 2–11 was set to 100%). As the neutral *N*-glycans in peak 1 coeluted with free 2-AB, their relative abundance could not be assessed (NA). The single peak fractions were collected and analyzed by MALDI-TOF-MS. One possible structure of the major glycan species in each peak fraction is represented schematically. Its compounds are represented by the symbols proposed by the nomenclature committee of the Consortium for Functional Glycomics (black rectangle, GlcNAc; gray circle, mannose; gray triangle, fucose; white circle, galactose; black diamond, sialic acid; http://glycomics.scripps.edu/CFGnomenclature.pdf). The peak fractions marked with # (A) contained impurities unrelated to *N*-glycans. Asterisks designate glycans whose number of terminal negatively charged substituents (sialic acid residues) was confirmed by MALDI-TOF/TOF tandem MS.

MALDI-TOF-MS allowed for the identification of 61 different oligosaccharides (Table SI), of which the most abundant ones are shown in Figure 2B. Of the 61 glycans, 56 were of the complex type. Thirty-four carried one fucose residue (Fuc) which most probably was a core α6 Fuc as usually seen in wild-type CHO cell-derived glycoproteins. A small amount (fraction 1) of neutral *N*-glycans was eluted shortly before the remaining free 2-AB label. The major glycan among the neutral *N*-glycans was of the high mannose type and contained five mannoses (Figure 2B). The other glycans in fraction 1 were nonsialylated complex-type *N*-glycans with or without one fucose. The negative charges on the glycans in the later eluting fractions were mostly due to sialic acid as evidenced by MALDI-TOF/TOF tandem MS analysis. The only exception was a phosphorylated species identified in peak 4 ($PhosHex_6HexNAc_2$; Table SI), probably corresponding to $PhosMan_6GlcNAc_2$ (Man-6-P). Peaks 3 and 4 contained 55% of all glycans, and the most abundant glycans in these peak fractions according to MALDI-TOF peak heights carried two sialic acid residues. Peaks 5–8 represented 22% of the *N*-glycans and the most prominent peaks in the corresponding MALDI-TOF spectra could be assigned to *N*-glycans carrying three sialic acid residues. The glycans contained in peak 2 (15%) and peaks 9–11 (9%) were of similar abundance and contained monosialylated and mostly tetrasialylated *N*-glycans, respectively. The largest glycans found were the fully sialylated, fucosylated tetraantennary structures with one or two *N*-acetyllactosamine repeats contained in fractions 8 and 9. Interestingly, the most abundant glycan contained in fraction 8 carried three *N*-acetylneuraminic acid (NeuAc) residues on only two antennae, and the predominant glycan in fraction 11 carried four NeuAc residues on maximally three antennae (Figure 2B). In some mono-, bi-, tri-, and tetrasialylated glycans, one NeuAc was replaced by *N*-glycolylneuraminic acid (NeuGc; Table SI). The relative amounts (as judged from the peak heights in the MALDI-TOF-MS) of the glycans with one NeuGc compared with the corresponding glycans carrying only NeuAc were estimated to ~16% in the monosialylated glycans, 24–30% in the disialylated, 44% in the trisialylated, and 51% in the tetrasialylated glycans (data not shown). Interestingly, the relative amount of the NeuGc-carrying variant of the tetrasialylated glycan with maximally three antennae from fraction 11 amounted to only ~32%.

N-Glycosylation sites of mouse sICAM-1 expressed in the Lec1 mutant of CHO cells

To understand how N-glycosylation influences the biological function of a protein on the molecular level, it is indispensable not only to elucidate the composition and structures of the *N*-glycans but also to identify the sites on the protein that are glycosylated. Mouse sICAM-1 contains nine potential N-glycosylation sites (Figure 3A). For the identification of the ones that are glycosylated, we used two complementary high-resolution MS approaches: (1) nanoLC-FTICR-MS of sICAM-1 trypsinized in solution and (2) direct MALDI-FTICR-MS of sICAM-1 treated with the endoglycosidases endoglycosidase H (Endo H) or PNGase F and trypsinized in silver-stained SDS–PAGE

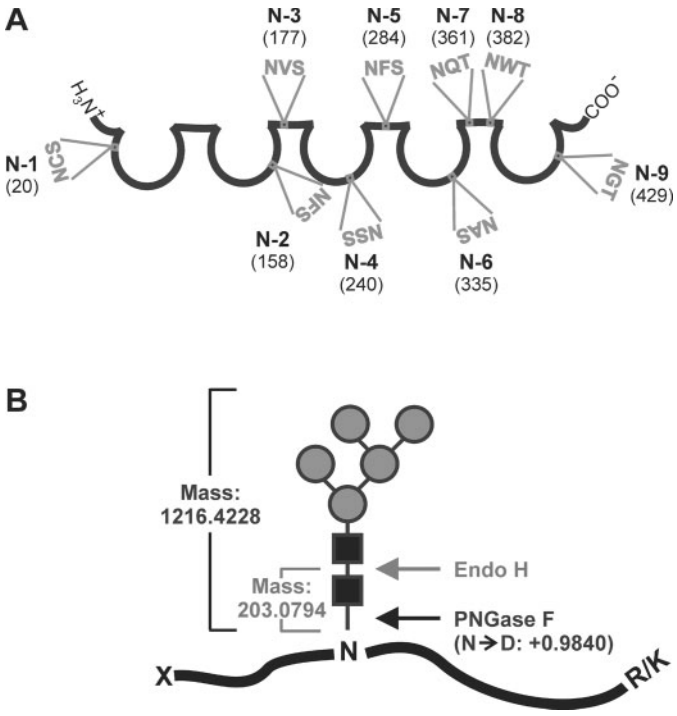

Fig. 3. Schematic representations of mouse sICAM-1, its nine potential N-glycosylation sites, and the strategies used for identification of the N-glycosylated sites. (**A**) Schematic representation of mouse sICAM-1. The five open circles symbolize the five Ig domains and the connecting straight lines the interdomain interfaces. The positions (amino acid number) and amino acid sequences of the nine potential N-glycosylation sites (N-1 to N-9) are shown. (**B**) To identify the N-glycosylation sites of mouse sICAM-1, we used sICAM-1 expressed in Lec1 cells, which carries only high mannose-type *N*-glycans, as a sample. The scheme shows the cleavage sites of Endo H and PNGase F and the corresponding mass increments to be expected for glycosylated tryptic peptides. Symbolic representation of monosaccharides is as in Figure 2B.

gels. All experiments were carried out with affinity-purified sICAM-1 expressed in the Lec1 mutant of CHO cells. The Lec1 mutant of CHO cells has a single insertion mutation that generates an inactive, truncated *N*-acetylglucosamine (GlcNAc) transferase I. Lec1 cells hence stop processing *N*-glycans at the $Man_5GlcNAc_2$-Asn stage (Stanley and Chaney, 1985; Chen and Stanley, 2003). sICAM-1 expressed in Lec1 cells has the following analytical advantages: (1) its glycosylation is more homogeneous than the glycosylation of sICAM-1 expressed in wild-type CHO cells (Otto *et al.*, 2004) and (2) being of the high mannose-type, its glycans are sensitive to Endo H which cleaves the glycosidic linkage between the two GlcNAcs of the chitobiose core leaving one GlcNAc residue on the protein (Figure 3B).

For analysis by nanoLC-FTICR-MS, sICAM-1 from Lec1 cells was reduced and alkylated in solution and then digested with trypsin and the resulting (glyco-) peptide mixture was directly injected into a nanoLC C18 column coupled to a Finnigan LTQ-FTICR mass spectrometer. The FTICR-MS data allowed to identify the glycosylated peptides comprising N-1, N-2, N-3, N-6, N-7, N-8, and N-9 (Figure 4, Table I), and the presence of $Hex_5HexNAc_2$ glycans was confirmed by MS/MS analysis (data not shown). As sICAM-1 from Lec1 cells could theoretically carry glycans with five to nine mannoses depending on whether the action of mannosidase I went to completion or not, we elucidated the masses and composition of the *N*-glycans of sICAM-1 expressed in Lec1 cells. *N*-Glycans were released by PNGase F treatment and then directly analyzed by MALDI-FTICR-MS (Figure 5A). The largest *m*/*z* measured was 1257.43161, which is in good agreement with the calculated *m*/*z* of the $[M + Na]^+$ ion of $Hex_5HexNAc_2$ (Δm = 6.8 ppm). Hence, sICAM-1 expressed in Lec1 cells only carries glycans of the composition $Man_5GlcNAc_2$.

Next, the reduced and alkylated band of sICAM-1 isolated by SDS–PAGE was subjected to in-gel deglycosylation with either PNGase F or Endo H, then to proteolysis by trypsin, and the resulting (glyco-) peptide mixtures were directly analyzed by MALDI-FTICR-MS. Figure 5B shows a MALDI-FTICR-MS of the peptide mixture obtained after deglycosylation with Endo H, which provided the identification of the peptides comprising the glycosylation sites N-2, N-3, N-4, N-5, N-6, N-7, and N-8 each carrying one remaining GlcNAc (Table II). Six of the seven glycopeptides were also found with the expected deamidated N-residues after PNGase F treatment (Table II). Taken together, the results from the two complementary high-resolution MS approaches show that all nine consensus sequences for N-glycosylation of mouse sICAM-1 are glycosylated.

Discussion

In a previous study, we showed that sialylated and galactosylated complex-type *N*-glycans as synthesized by wild-type CHO cells strongly enhance the ability of mouse sICAM-1 to induce MIP-2 production in astrocytes (Otto *et al.*, 2004). The present study was aimed at defining the sialylation and structures of the function-enhancing glycans of mouse sICAM-1 expressed in wild-type CHO cells as well as the sites on mouse sICAM-1 which are N-glycosylated.

For defining the sialylation and structures of highly complex mixtures of glycans, combinations of chromatography with high-sensitivity MS methods have proven to be particularly powerful (Dell and Morris, 2001). The method used here for profiling of the sialylated *N*-glycans of mouse sICAM-1 was based on enzymatic *N*-glycan release, fluorescent labeling of the reducing end, separation, and analysis by fluorometric HP-IEC and MALDI-TOF-MS. This analysis showed that the majority of *N*-glycans of mouse sICAM-1 from wild-type CHO cells were of the sialylated complex type, confirming earlier data based on IEF after neuraminidase treatment, SDS–PAGE after Endo H treatment, and monosaccharide compositional analysis (Otto *et al.*, 2004). HP-IEC separated these glycans according to charge (number of sialic acid residues) and according to the size/number of *N*-acetyllactosamine units (Figure 2B). All charged groups were due to sialic acid with the only exception of one phosphorylated glycan ($PhosHex_6HexNAc_2$, probably corresponding to $PhosMan_6GlcNAc_2$/Man-6-P) in fraction 4 (Table SI). The phosphorylated glycotope Man-6-P is the key structural determinant in targeting glycoproteins to the lysosomal compartment but is also found

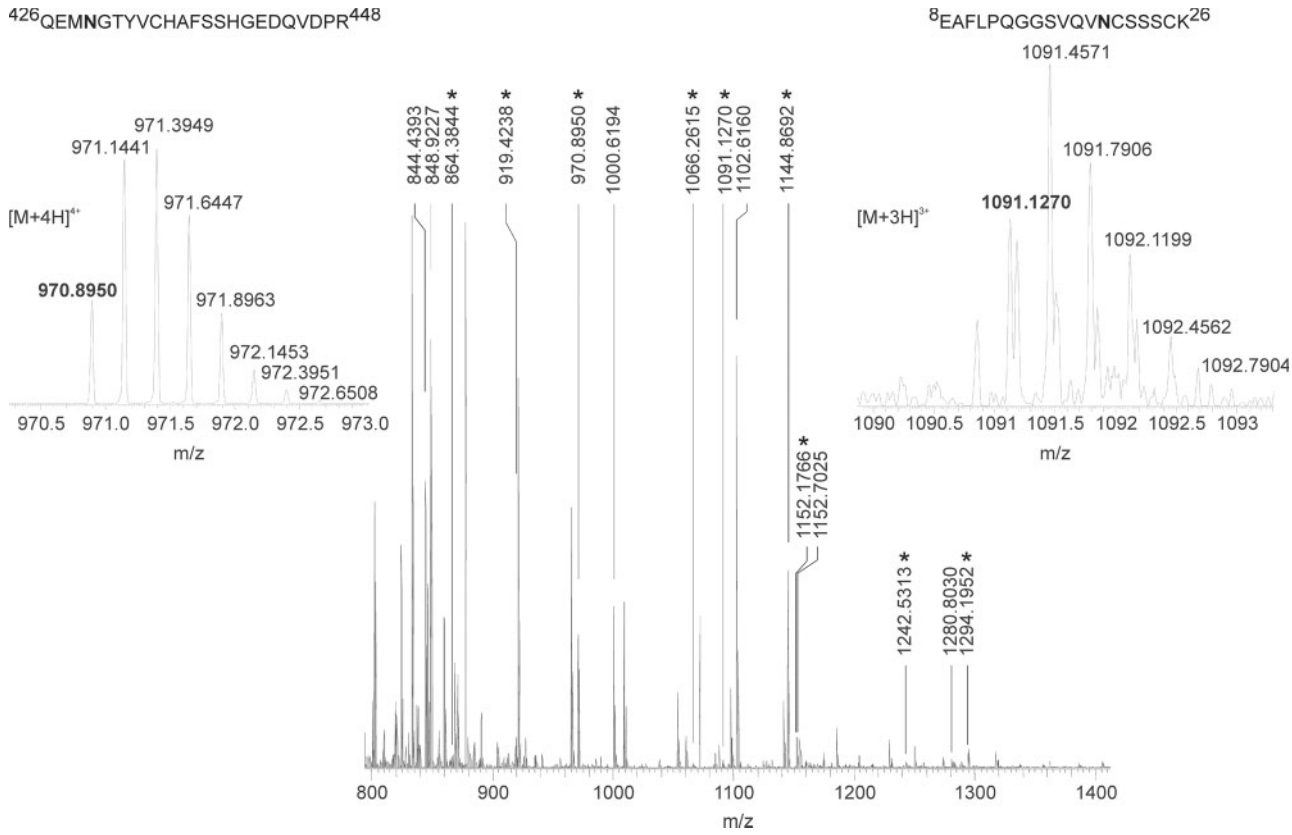

Fig. 4. Full-scan ESI-FTICR-MS of the tryptic (glyco-) peptide mixture of mouse sICAM-1 expressed in Lec1 cells. Purified sICAM-1 from Lec1 cells was reduced, alkylated, and digested with trypsin in solution. The resulting (glyco-) peptide mixture was injected into a nanoLC column coupled to a hybrid LTQ-FTICR mass spectrometer. Exact monoisotopic masses of the ions detected are shown above the peaks. For assignment of peptides carrying a $Hex_5HexNAc_2$ glycan (highlighted by asterisks), see Table I. The insets show the isotopic distributions of the $[M + 4H]^{4+}$ ion of the glycopeptide (426–448) and of the $[M + 3H]^{3+}$ ion of the glycopeptide (8–26) containing the N-9 and N-1 glycosylation sites, respectively.

Table I. NanoLC-FTICR-MS identification of tryptic peptides containing N-glycosylation sites carrying $Hex_5HexNAc_2$ glycans (m/z 1216.4228)

Position of N-glycosylation site (amino acid number)	Tryptic glycopeptides					Additional modification
	Position of peptide	m/z_{calc}	m/z_{obs}	Charge state (z)	$\Delta m/z$ (ppm)	
N-1 (20)	8–26	1091.1220	1091.1270	3+	4.58	Alkylation (C-21, C-25)
N-2 (158)	143–162	864.3797	864.3844	4+	5.44	Alkylation (C-161)
N-2 (158)	143–162	1152.1704	1152.1766	3+	5.38	Alkylation (C-161)
N-3 (177)	163–182	1144.8687	1144.8692	3+	0.43	
N-6 (335)	315–342	1066.2618	1066.2615	4+	0.28	
N-7 (361)	361–373	919.4223	919.4238	3+	1.63	
N-8 (382)	374–394	1242.5230	1242.5313	3+	6.68	Alkylation (C-379)
N-9 (429)	426–448	970.8918	970.8950	4+	3.30	Alkylation (C-434)
N-9 (429)	426–448	1294.1864	1294.952	3+	6.80	Alkylation (C-434)

on recombinant glycoproteins with high expression levels (Varki *et al*., 1999; Lee *et al*., 2003). Besides this phosphorylated high mannose-type *N*-glycan, the only *N*-glycans not being of the complex type were a small amount of neutral high mannose-type *N*-glycans found in fraction 1. These high mannose-type *N*-glycans probably derive from a small amount of sICAM-1 carrying only high mannose-type *N*-glycans detected in our previous study and probably represent incompletely processed *N*-glycans (Otto *et al*., 2004). The complex-type *N*-glycans of sICAM-1 ranged from

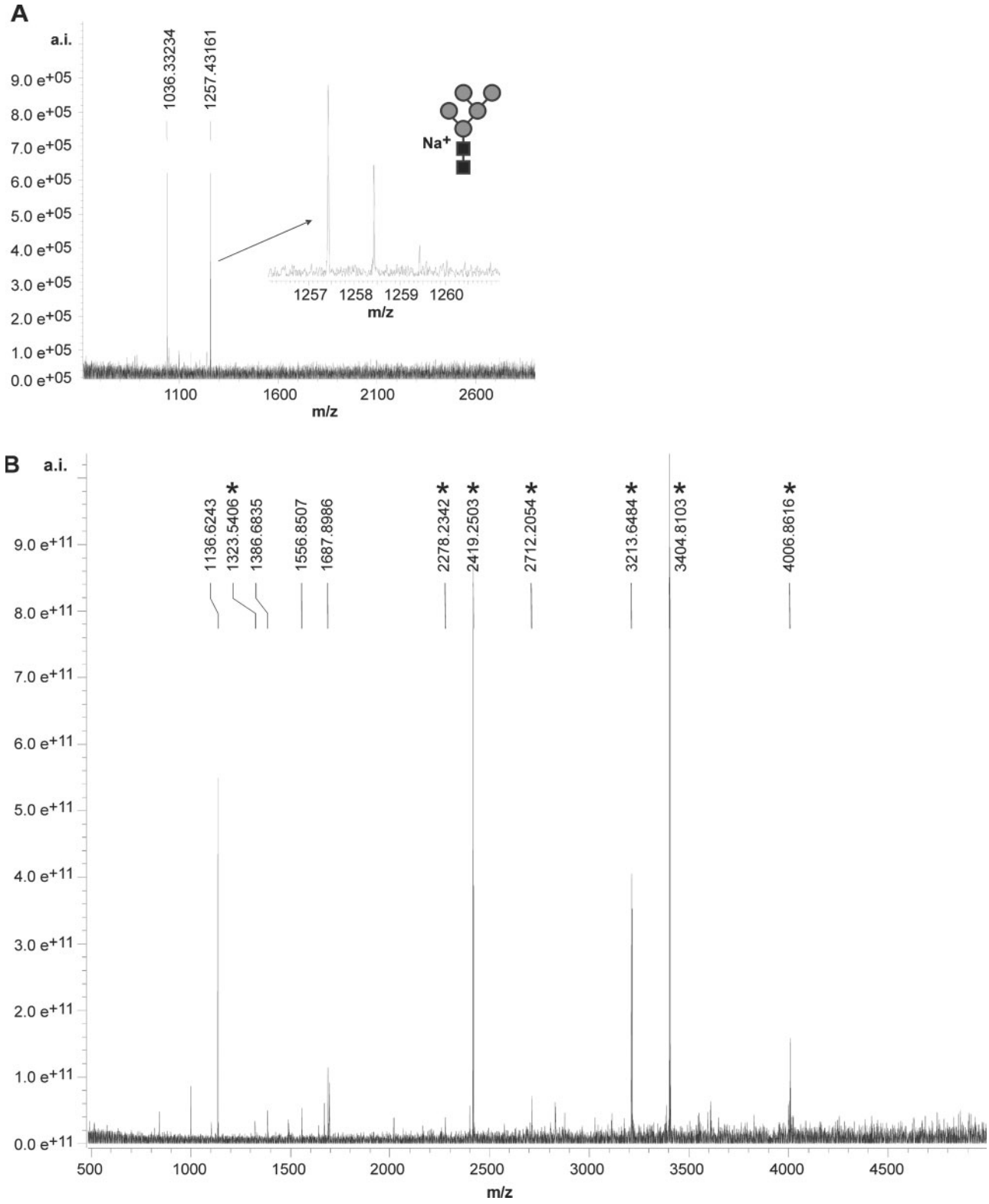

Fig. 5. MALDI-FTICR-MS of the *N*-glycans of mouse sICAM-1 from Lec1 cells and of the tryptic (glyco-) peptide mixture obtained after Endo H treatment. (**A**) *N*-Glycans from mouse sICAM-1 expressed in Lec1 cells were released by PNGase F treatment, purified over Carbograph, and analyzed by MALDI-FTICR-MS. The inset shows the monoisotopic peak of the largest *m*/*z* detected, that is, 1257.43161 corresponding to the depicted $Hex_5HexNAc_2$ with a Na^+ adduct (calculated *m*/*z* of the $[M + Na]^+$ ion: 1257.4231, Δm = 6.8 ppm). The *m*/*z* 1036.33234 can be assigned to the same glycan having lost one HexNAc at its reducing end. Symbolic representation of monosaccharides is as in Figure 2B. (**B**) Purified sICAM-1 from Lec1 cells was isolated by SDS–PAGE, reduced, alkylated, and digested in gel with Endo H followed by trypsin and analyzed by MALDI-FTICR-MS. Exact monoisotopic *m*/*z* values of $[M + H]^+$ ions are shown above the peaks. For assignment of peptides carrying one GlcNAc residue after Endo H treatment (highlighted by asterisks), see Table II.

Table II. MALDI-FTICR-MS identification of tryptic peptides carrying one GlcNAc residue (*m/z* 203.0794) at the N-glycosylation site after Endo H treatment or having deamidated N-residues (+*m/z* 0.9840) after deglycosylation with PNGase F

Position of N-glycosylation site (amino acid number)	Position of peptide	Tryptic peptides after Endo H treatment			Tryptic peptides after PNGase F treatment			Additional modification
		$[M + H]^+_{calc}$ (*m/z*)	$[M + H]^+_{obs}$ (*m/z*)	Δ*m/z* (ppm)	$[M + H]^+_{calc}$ (*m/z*)	$[M + H]^+_{obs}$ (*m/z*)	Δ*m/z* (ppm)	
N-2 (158)	153–162	1323.5388	1323.5406	1.4				Alkylation (C-161)
N-3 (177)	163–182	2419.2469	2419.2503	1.4	2217.1516	2217.1477	1.7	
N-4 (240)	225–259	4006.8604	4006.8616	0.3	3804.7650	3804.7397	6.6	
N-5 (284)	279–306	3213.6783	3213.6484	9.3	3011.5829	3011.5701	4.2	
N-6 (335)	315–343	3404.7815	3404.8103	8.4	3202.6861	3202.6757	3.2	
N-7 (361)	357–373	2278.2236	2278.2342	4.6	1540.8124	1540.8082	2.7	
N-8 (382)	374–394	2712.2100	2712.2054	1.7	2510.1146	2510.1167	0.8	Alkylation (C-379)

small biantennary to large tetraantennary structures with two *N*-acetyllactosamine repeats. Of the 61 *N*-glycan structures identified, 34 contained one fucose and 28 two or three sialic acid residues. Interestingly, a significant fraction (~4% according to HP-IEC peak area and MALDI-TOF peak height) was found to carry a higher number of sialic acid residues than of antennae. The additional sialic acid residues can theoretically be attached either to subterminal GlcNAc residues in α2,6 linkage as seen on mouse transferrin (Coddeville *et al*., 2000) or to a terminal sialic acid in α2,8 linkage, forming di/oligosialic acid. We favor the latter interpretation because CHO cells are known to express the polysialyltransferase ST8SiaIV responsible for the synthesis of di/oligosialic acid (Muhlenhoff *et al*., 2001) but have never been reported to attach α2,6-linked sialic acid to subterminal GlcNAc residues. A disialic acid motif often terminates the oligosaccharide chains of gangliosides but was also found on glycoproteins derived from mammalian brain (Sato *et al*., 2000). The function of di- and oligosialic acids on glycoproteins is presently unclear. One study demonstrated that disialic acid on *O*-glycans of CD166 may be involved in neurite outgrow (Sato *et al*., 2002). Another study demonstrated that the integrin α_5 subunit carries oligosialic acid and that oligosialic acid is required for the adhesion of the integrin α_5 subunit to fibronectin (Nadanaka *et al*., 2001). Lectins that specifically bind disialic acid were recently described. Human siglec-11 occurring on macrophages in various tissues and on microglia was found to specifically recognize α2,8-linked sialic acid (Angata *et al*., 2002) and mouse siglec-E expressed on neutrophils bound preferentially to sialic acid in α2,8 linkage (Zhang *et al*., 2004).

In some of the more abundant, mostly fucosylated mono-, di-, tri-, and tetrasialylated glycans of sICAM-1, one NeuAc residue was replaced by a NeuGc residue. NeuGc is found on glycoproteins of virtually all vertebrates, except for humans and chicken (Chenu *et al*., 2003). In animals, NeuGc is formed as the sugar nucleotide cytidine monophosphate-*N*-glycolylneuraminic acid (CMP-NeuGc) by the action of CMP-NeuAc hydroxylase, an enzyme which is inactivated through the loss of an exon in humans (Chenu *et al*., 2003). The relative amounts of the sICAM-1-derived *N*-glycans carrying one NeuGc as compared with the corresponding glycan carrying only NeuAc suggest that ~13% of the total CMP-sialic acid available for sialylation in wild-type CHO cells is NeuGc. Interestingly, the relative amount of the NeuGc-carrying isoform of the tetrasialylated triantennary glycan probably containing the di/oligosialic acid motif was only ~32% suggesting some selectivity for CMP-NeuAc in di/oligosialic acid synthesis by wild-type CHO cells.

The glycosylation of mouse sICAM-1 from wild-type CHO cells presented here is similar to the glycosylation of human sICAM-1 from wild-type CHO cells (Bloom *et al*., 1996) in that both glycoproteins carry mostly heavily sialylated, fucosylated complex-type *N*-glycans. In contrast to human sICAM-1, mouse sICAM-1 seems not to carry any hybrid-type *N*-glycans. Furthermore, the presence of *N*-glycans with more sialic acid residues than antennae (probably carrying di/oligosialic acid) seems to be a characteristic feature of mouse sICAM-1, which is not found on human sICAM-1. The enhanced ability of sialylated mouse sICAM-1 from wild-type CHO cells to induce MIP-2 production may hence be due to a high extent of sialylation, the presence of the di/oligosialic acid motif, and/or the variety of large complex-type *N*-glycans with terminal negatively charged sialic acid residues (Figure 6). A high extent of sialylation could protect sICAM-1 from uptake by the mannose receptor into astrocytes, thereby prolonging the interaction time of sICAM-1 with its astrocytic receptor. A high number of negatively charged sialic acid residues could also alter the conformation of sICAM-1 and/or its recognition by the receptor in a function-enhancing manner. If the fraction of glycans probably containing di/oligosialic acid were to contribute to the increase in MIP-2-inducing activity, specific recognition by the astrocytic receptor would be a probable mechanism. Another possibility is that the variety and complexity of the sialylated *N*-glycans are recognized by astrocytic cell surface proteins in a manner that is comparable to pattern recognition by innate immunity receptors and that this pattern recognition is translated into enhanced MIP-2 induction.

To understand how glycosylation may influence the biological function of a protein, we need to know not only the

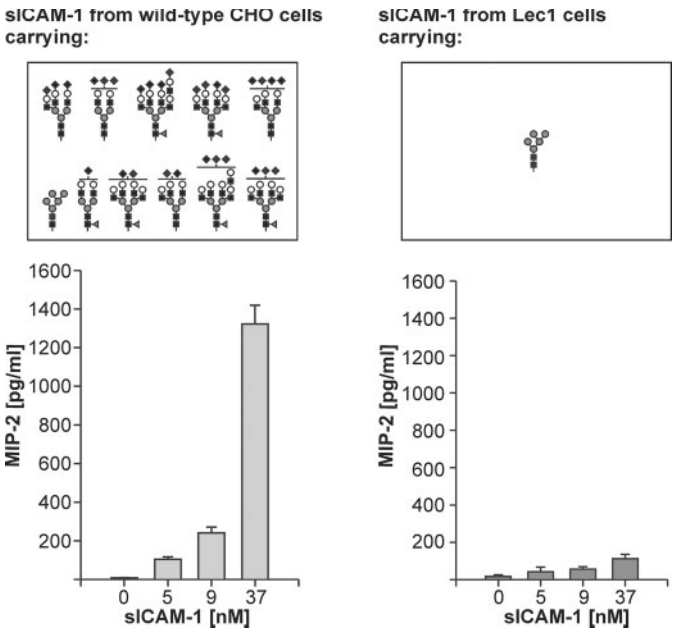

Fig. 6. The ability of mouse sICAM-1 to induce MIP-2 production in astrocytes and how it is influenced by glycosylation. The *N*-glycans present on mouse sICAM-1 expressed in wild-type CHO cells and in the Lec1 mutant of CHO cells as determined in the present study are juxtaposed to the MIP-2-inducing activities of the two sICAM-1 glycoforms as determined in our previous study (Otto *et al*., 2004). To determine the MIP-2-inducing activity, we treated primary mouse astrocytes with increasing concentrations of purified sICAM-1 expressed in either wild-type CHO or Lec1 cells. After 24 h, the culture supernatants were harvested, and secreted MIP-2 was measured by enzyme-linked immunosorbent assay. The data are presented as average ± SD of four assays derived from two independent experiments, each performed in duplicate.

structures and relative amounts of the glycans but also the sites on the protein that are glycosylated. Therefore, we analyzed which of the nine consensus sequences for N-glycosylation of mouse sICAM-1 expressed in the Lec1 mutant of CHO cells carry *N*-glycans. For this purpose, we used two complementary high-resolution MS approaches: nanoLC-ESI-FTICR-MS of sICAM-1 trypsinized in solution and direct MALDI-FTICR-MS of sICAM-1 which had been treated with Endo H or PNGase F and trypsinized in silver-stained SDS–PAGE gels. The combination of these approaches led to the discovery that all nine potential N-glycosylation sites of mouse sICAM-1 from Lec1 cells were actually glycosylated with $Man_5GlcNAc_2$.

All previous studies on the glycosylation of ICAM-1 were performed using human sICAM-1. Five consensus sequences for N-glycosylation are conserved between human and mouse ICAM-1 (N-156/158, N-175/177, N-240, N-358/361, N-379/382). One previous study based on reversed-phase-HPLC and ESI-MS of tryptic peptides showed that all eight N-glycosylation sites of human ICAM-1 were glycosylated (Bloom *et al*., 1996). Another study based on crystallization and electron density maps of Endo H-treated domains 3–5 of human ICAM-1 expressed in Lec3.2.8.1 cells reported that N-379 was not glycosylated and that this was probably due to the unfavorable presence of a tryptophan in the NWT N-glycosylation sequon (Yang *et al*., 2004). Here, the glycosylation site corresponding to human N-379, N-8 (382) was glycosylated although the NWT N-glycosylation sequon is conserved in the mouse protein.

The glycosylation sites on domain 3 of human ICAM-1 were previously reported to be important for binding to Mac-1. Large complex-type glycans at N-240 and N-269 inhibited the binding of human ICAM-1 to Mac-1 (Figure 1; Diamond *et al*., 1991). Interestingly, N-240 is conserved in mouse sICAM-1, whereas the N-glycosylation site that had an even larger impact on binding of human ICAM-1 to Mac-1, N-269 is not.

The potential N-glycosylation sites of human ICAM-1 are all located in the middle part of the molecule (between domain 2 and the interdomain interface following domain 4), whereas mouse sICAM-1 additionally has potential N-glycosylation sites in the first (N-1) and the fifth Ig-like domain (N-9). N-1 is of particular interest, as it is located close to the binding site of LFA-1. Even though absent in human ICAM-1, it is present in all other members of the human ICAM family (ICAM-2 to ICAM-5; Jimenez *et al*., 2005). The crystal structure of human ICAM-2 showed that the first GlcNAc at N-1 interacted with the tryptophan residue W51. Both N-1 and the interacting tryptophan residue (glycan1-W motif) are highly conserved in the ICAM subfamily. The only ICAM subfamily members not having a glycan1-W motif are ICAM-1 from humans and chimpanzees. Interestingly, when human ICAM-1 was mutated to contain the glycan1-W motif (T20N, R49W), its binding to LFA-1 was not altered (Jimenez *et al*., 2005). In contrast, the binding of ICAM-2 and ICAM-3 to LFA-1 was abolished when the glycan1-W motif was eliminated by site-directed mutagenesis (Klickstein *et al*., 1996; Jimenez *et al*., 2005). It may therefore be that the presence of a glycan containing at least one GlcNAc at N-1 and of W-48 is required for a proper folding of domain 1 of mouse sICAM-1 allowing for binding to LFA-1.

The induction of MIP-2 production by mouse sICAM-1 in astrocytes occurs by binding to an as yet undefined receptor and is enhanced by sialylated complex-type *N*-glycans. Because neither the astrocytic receptor nor its binding site on sICAM-1 are known, further research should be aimed at defining whether enhanced MIP-2 induction is due to the sialylated glycans attached to a specific N-glycosylation site or to a specific protein conformation stabilized by the glycosylation of the nine N-glycosylation sites with the sialylated *N*-glycans described here.

The glycosylation of the nine N-glycosylation sites of mouse sICAM-1 from Lec1 cells can be expected to occur also on mouse sICAM-1 from natural sources, as the occupancy of N-glycosylation sites is determined by their protein environment (Petrescu *et al*., 2004). The observation of changes in sialylation and galactosylation of *N*-glycans altering the ability of recombinant mouse sICAM-1 from wild-type CHO cells to induce MIP-2 production leads to the hypothesis that the MIP-2-inducing activity of sICAM-1 may also be regulated by glycosylation *in vivo*. Glycosylation by wild-type CHO cells is similar to glycosylation in mice in various aspects (e.g., the synthesis of NeuGc, α2,8-linked disialic acid; Yasukawa *et al*., 2006) and differs in others (e.g., the absence of α2,6-linked sialic acid and of

antenna fucosylation). It will be interesting to extend the analysis of the N-glycosylation of mouse sICAM-1 expressed in wild-type CHO cells performed here to mouse sICAM-1 present in mouse brain and serum under normal and under inflammatory conditions. Inflammatory stimuli have been shown to up-regulate the expression of glycosyltransferases that are responsible for the biosynthesis of sialylated *N*-glycans, and an increased expression of sialylglycotopes on serum glycoproteins was found in response to turpentine oil-induced inflammation in mice (Delmotte *et al.*, 2002; Garcia-Vallejo *et al.*, 2005; Yasukawa *et al.*, 2005). If an increase in (α2,3 and/or α2,8-linked) sialylation of sICAM-1 in serum and/or brain of mice with experimental brain trauma was observed, it may in fact be that MIP-2 induction is regulated by the sialylation of mouse sICAM-1 after brain trauma.

Materials and methods

Materials

PNGase F (catalog number 1 365 193) and Endo H (catalog number 1 088 726) were purchased from Roche Diagnostics GmbH (Penzberg, Germany). The Signal 2-AB labeling kit (GKK-404), the GlycoSep C column (I-4721), and GlycoClean S cartridges (GKI-4726) were obtained from Prozyme-Glyko (San Leandro, CA). Carbograph SPE columns were purchased from Alltech Associates (Deerfield, IL). NuTip graphitized carbon 10-μL pipette tips were from Glygen (Columbia, MD). Trifluoroacetic acid (TFA) and 5-methoxysalicylic acid were purchased from Sigma-Aldrich (St. Louis, MO). 2,5-Dihydroxybenzoic acid (DHB) puriss. p.a. was from Fluka (Buchs, Switzerland). Sequencing grade trypsin was purchased from Promega (Mannheim, Germany).

Preparation of sICAM-1 expressed in wild-type CHO and Lec1 cells

The extracellular portion of mouse ICAM-1 with the 12-amino acid HPC4 epitope tag attached to its C-terminus after G441 was expressed in either dihydrofolate reductase-deficient CHO cells (designated as wild-type CHO) or the Lec1 mutant of CHO cells and affinity-purified from culture supernatants as previously described (Otto *et al.*, 2004). Eluted sICAM-1 was dialyzed against three changes of low-salt TBS (5 mM Tris–HCl, pH 7.5, 15 mM NaCl) and concentrated 10–20-fold with a Centricon 30 concentrator (Millipore, Billerica, MA). The concentrations of the two sICAM-1 glycoforms were assessed by western blot analysis and comparison to an sICAM-1 standard of known concentration (Otto *et al.*, 2004).

Release and purification of N*-glycans from sICAM-1 expressed in wild-type CHO and Lec1 cells*

An aliquot containing 1 nmol of sICAM-1 expressed in either wild-type CHO or Lec1 cells was lyophilized and dissolved in 8.2 μL of ultrapure water. Then, sICAM-1 was denatured by boiling for 10 min in 0.5% sodium dodecyl sulfate (SDS) and 1% β-mercaptoethanol. Nonidet P-40 (NP-40) was added in 7.5× excess of SDS. The *N*-glycans were released from the protein by PNGase F treatment, using 525 U/mL of enzyme for 2 nmol/mL (corresponding to ~190 μg/mL) of sICAM-1 from wild-type CHO cells and 315 U/mL of enzyme for 2 nmol/mL (corresponding to ~125 μg/mL) of sICAM-1 from Lec1 cells in phosphate-buffered saline pH 7.4, and incubating for 21 h at 37 °C. The completeness of *N*-glycan release was confirmed by SDS–PAGE and western blot analysis (Otto *et al.*, 2004). The released *N*-glycans were separated from the proteins and other contaminants (salts, detergents, and reagents) using nonporous graphitized carbon black Carbograph SPE columns (150 mg, corresponding to a bed volume of ~0.5 mL) as previously described (Packer *et al.*, 1998). Briefly, columns were conditioned with three bed volumes of 80% (v/v) acetonitrile (ACN) containing 0.1% (v/v) TFA followed by three bed volumes of ultrapure water. Samples were loaded onto the columns, and glycans were left to adsorb to the carbon for 1–2 min. Contaminants were washed off with three bed volumes of ultrapure water, and glycans were eluted with three bed volumes of 25% (v/v) ACN containing 0.05% (v/v) TFA. Flow was generated by gravity and was between 0.5 and 1 mL/min. The eluates were lyophilized and stored at –20°C.

Preparation of fluorescently labeled N*-glycans from sICAM-1 expressed in wild-type CHO cells*

The glycan pool of sICAM-1 from wild-type CHO cells was reductively aminated with 2-AB (molecular weight 136.15) using the Signal 2-AB labeling kit, according to the manufacturer's instructions. Briefly, the lyophilized sample was dissolved in 5 μL of a solution of 2-AB (0.35 M) and sodium cyanoborohydride (1 M) in 30% (v/v) acetic acid in dimethylsulfoxide (DMSO). After incubation at 65°C for 3 h, the excess reagents were separated from the labeled glycans using a GlycoClean S cartridge, following the manufacturer's instructions. The oligosaccharide solution was then filtered through an IC Millex-LG Filter Unit (Millipore, Billerica, MA; pore size 0.2 μm), lyophilized, and stored protected from light at –20°C.

HP-IEC of fluorescently labeled N*-glycans*

HP-IEC analyses were performed on a Merck Hitachi LaChrom D-7000 system (Merck KGaA, Darmstadt, Germany/Hitachi High Technologies America, San Jose, CA) equipped with a fluorescence detector L-7480. The dried 2-AB-labeled oligosaccharides from sICAM-1 expressed in wild-type CHO cells were dissolved in 250 μL of water. A 50-μL aliquot of this solution, undiluted or 4-fold diluted, was injected onto the GlycoSep C HP-IEC column, and the 2-AB-labeled glycans were separated at room temperature using a flow rate of 0.4 mL/min and an ACN/water/ammonium acetate gradient as modified from the work of Viseux and others (2001). In a first step, the ACN content was decreased from 80 to 20% within 13 min, whereas the water proportion was increased accordingly. In a second step, in which ACN was kept constant at 20%, the concentration of ammonium acetate (pH 4.5) was increased from 0 to 160 mM in 35 min. The eluate was monitored by fluorescence detection (λ_{ex} 330 nm, λ_{em} 420 nm). A Merck-Hitachi Model D-7000 Chromatography Data Station software version 4.0

was used for recording the spectra and for calculating the peak areas. Peak fractions were collected, lyophilized, and stored at –20°C.

MALDI-TOF-MS of chromatographic fractions

The peak fractions collected from HP-IEC were desalted prior to MS analysis using NuTip graphitized carbon 10-μL pipette tips (Glygen, Columbia, MD). Tips were conditioned by pipetting five times 10 μL of 60% (v/v) ACN containing 0.05% (v/v) TFA followed by three times 10 μL of water. Dried HP-IEC fractions were dissolved in 5 μL of water. Samples were bound to the carbon by pipetting up and down 50 times 2 μL volumes (20 times oversampling). Contaminants were washed off by pipetting 10 times 10 μL of water, and glycans were eluted with five times 1.5 μL of 60% (v/v) ACN containing 0.05% (v/v) TFA. Each 1.5 μL aliquot of eluent was pipetted up and down 10 times before collection of the eluate. Samples were then vacuum dried.

MALDI-TOF-MS was carried out using a 4700 Proteomics Analyzer (Applied Biosystems, Foster City, CA) equipped with a nitrogen UV laser (λ_{max} 337 nm). Mass spectra were recorded at matrix-optimized laser fluency, with an accelerating voltage of 20 kV and in negative polarity linear mode. The spectra were obtained by summation of 50 subspectra, each averaged over 50 laser shots. Dried, desalted HP-IEC fractions were dissolved in 2 μL of 70% (v/v) methanol and mixed with 2 μL of superDHB matrix solution (9:1 mixture of 20 mg/mL DHB and 20 mg/mL 5-methoxysalicylic acid in 70% methanol, containing 10 mM ammonium citrate). After the transfer of 1.4 μL of this mixture to the target, the solution was allowed to dry at ambient temperature and pressure. External on-plate mass calibration in the *m/z* range 750–4250 was performed using a reference peptide mixture (Applied Biosystems). The MALDI-TOF procedure was optimized for sensitivity, resolution, and minimal sialic acid loss using a 2-AB-labeled trisialylated triantennary reference *N*-glycan (A3; Dextra, Reading, UK). Of the more abundant components, the number of terminal negatively charged substituents was confirmed by MALDI-TOF/TOF tandem MS at 1 keV collisional energy in the negative-ion mode, using air at $5.10E^{-7}$ Torr as the collision gas. Control analyses as above were conducted with 1 nmol of human α-1 acid glycoprotein (Sigma).

Tryptic digestion of sICAM expressed in Lec1 cells in solution

A 100-μg sample of sICAM expressed in Lec1 cells was reduced for 45 min at 56°C in 270 μL of 50 mM ammonium bicarbonate containing 5.5 mM dithiothreitol (DTT) and then S-alkylated for 1 h at 20°C in the dark by adding 30 μL of 100 mM iodoacetamide (IAA) to a final concentration of 10 mM IAA. Trypsin was added in a final enzyme:substrate ratio of 1:50, and the digestion was carried out for 2 h at 37 °C. The reaction was stopped by freezing the sample with liquid nitrogen. The tryptic digest was then lyophilized and redissolved in 2% ACN in 0.1% TFA just prior to nanoLC-MS/MS analysis.

NanoLC-MS/MS

NanoLC-MS/MS experiments were performed on a Finnigan LTQ-FT hybrid linear ion trap/7T FTICR mass spectrometer (Thermo Electron, San Jose, CA), equipped with a Finnigan Nanospray ion source (Thermo Electron), a Finnigan Surveyor MS pump (Thermo Electron), and a Finnigan micro-autosampler (Thermo Electron). The sICAM-1 tryptic peptide mixture was separated on a 50-μm ID PicoFrit column packed in-house with Magic C18AQ material (Michrom BioResources, Auburn, CA). The column was packed to a length of 12 cm with a 100% MeOH slurry of C18 reversed-phase material (100 Å pore size, 3 μm particle size) using a high-pressure cell pressurized with helium. The column was equilibrated before sample injection for 10 min at 2% solvent B (0.1% [v/v] formic acid in ACN) and 98% solvent A (0.1% [v/v] formic acid in water) at a flow rate of 140 nL/min. Separation was achieved by using a linear gradient from 2 to 50% solvent B in 24 min at a flow rate of 320 nL/min. The LTQ-FT mass spectrometer was operated in the data-dependent acquisition mode using the TOP10 method: a full-scan MS acquired in the FTICR mass spectrometer was followed by 10 MS/MS experiments performed with the LTQ on the 10 most abundant ions detected in the full-scan MS.

Analysis of the N*-glycans from sICAM-1 from Lec1 cells by MALDI-FTICR-MS*

The *N*-glycan pool of sICAM-1 from Lec1 cells eluted from the Carbograph SPE column was directly analyzed by MALDI-FTICR-MS as described below.

In-gel deglycosylation and proteolytic digestion of sICAM-1 from Lec1 cells

The silver-stained band of sICAM-1 from Lec1 cells was excised from a 7.5% SDS–PAGE gel, washed, reduced with DTT, and S-alkylated with IAA as previously described (Shevchenko *et al.*, 1996). After reduction and alkylation, gel pieces were washed with 50–100 μL of 50 mM ammonium bicarbonate for 10 min, dehydrated by the addition of ACN, swelled by rehydration in 50 mM ammonium bicarbonate, and shrunk again by the addition of the same volume of ACN. The liquid phase was removed, and the gel pieces were dried in a vacuum centrifuge.

sICAM-1 was then treated in gel with Endo H or PNGase F. Although PNGase F treatment allows for easy identification of the deglycosylated peptides, Endo H treatment allows for a more secure identification of glycosylated peptides. The presence of a remaining GlcNAc is a more reliable sign of previous N-glycosylation than the transformation of asparagine into aspartic acid by PNGase F (Figure 3B), because such a transformation may also be due to spontaneous asparagine oxidation. For in-gel deglycosylation, the gel pieces were swollen in 50 μL of deglycosylation buffer containing either Endo H (500 mU/mL in 25 mM ammonium bicarbonate adjusted to pH 5.5 with HCl) or PNGase F (100 U/mL in 50 mM ammonium bicarbonate). If all the liquid was taken up by the gel pieces, further deglycosylation buffer (but without Endo H or PNGase F) was added to keep the samples wet during overnight incubation at 37°C (Kuster and Mann, 1999). To avoid interference from PNGase F- or Endo H-related peptides

in the MS spectra, the deglycosylation enzymes were removed prior to proteolysis as previously described (Kuster and Mann, 1999), but using ammonium bicarbonate at 50 mM (instead of 100 mM), and then the gel pieces were dried in a vacuum centrifuge.

The dried gel pieces were rehydrated in the protease solution (12.5 ng/μL of trypsin in 50 mM ammonium bicarbonate) at 4°C for 45 min. The supernatant solution was removed and replaced by 10–20 μL of 50 mM ammonium bicarbonate without protease to keep the gel pieces wet during overnight incubation (37°C) as previously described (Shevchenko *et al*., 1996). The supernatant was removed, lyophilized, and analyzed by MALDI-FTICR-MS. Protein fragments were additionally eluted from the gel pieces by shaking them twice with a mixture of one part 20 mM ammonium bicarbonate and two parts of ACN for 2 h at 20°C. The eluates were combined, lyophilized, and dissolved just before MALDI-FTICR-MS analysis in 5 μL of ACN/0.1% TFA in water (2:1).

MALDI-FTICR-MS

The tryptic digests of mouse sICAM-1 were directly analyzed by MALDI-FTICR-MS using a Bruker APEX II FTICR instrument equipped with an actively shielded 7T superconducting magnet (Magnex, Oxford, UK), a cylindrical infinity ICR analyzer cell, and an external Scout 100 fully automated *X–Y* target stage MALDI source with pulsed collision gas. A 100 mg/mL solution of DHB in ACN/0.1% TFA in water (2:1) was used as the matrix. A 0.5-μL aliquot of matrix solution and 0.5 μL of sample solution were mixed on the stainless-steel MALDI target and allowed to dry. The pulsed nitrogen laser was operated at 337 nm, and the ions generated by 20–30 laser shots were accumulated in the hexapole for 0.5–1 s. Mass spectra were obtained by the acquisition of typically 32–64 scans. External calibration was carried out using the monoisotopic masses of singly protonated ion signals of bovine insulin (5730.609), oxidized bovine insulin B-chain (3494.651), bee venom melittin (2845.762), human adrenocorticotropic hormone (ACTH) fragment (2465.199), human neurotensin (1672.917), human angiotensin I (1296.685), human bradykinin (1060.569), and human angiotensin II (1046.542). The acquisition and processing of spectra were performed with the XMASS software (Bruker Daltonics, Bremen, Germany).

Supplementary data

Supplementary data are available at Glycobiology online (http://glycob.oxfordjournals.org/). Table SI: supplementary mass spectrometric data to Figure 2.

Acknowledgments

We thank Matthias Meyer from the Institute of Pharmaceutical Sciences, ETH Zurich for excellent technical assistance with protein purification. We thank Dr. Catalina Damoc and Dr. Brett Phinney from UC Davis Proteomic Core Facility for expert help with Finnigan LTQ-FT mass spectrometer.

Conflict of interest statement

None declared.

Abbreviations

2-AB, 2-aminobenzamide; ACN, acetonitrile; CHO, Chinese hamster ovary; CMP, cytidine monophosphate; DHB, 2,5-dihydroxybenzoic acid; DTT, dithiothreitol; Endo H, endoglycosidase H; ESI, electrospray ionization; FTICR, Fourier transform ion cyclotron resonance; Fuc, fucose; Gal, galactose; GlcNAc, *N*-acetylglucosamine; HP-IEC, high-performance ion-exchange chromatography; IAA, iodoacetamide; ICAM-1, intercellular adhesion molecule-1; IEF, isoelectric focusing; LFA-1, leukocyte function-associated antigen-1; Mac-1, macrophage antigen-1; MALDI-TOF, matrix-assisted laser desorption ionization-time of flight; Man, mannose; MIP-2, macrophage inflammatory protein-2; MS, mass spectrometry; NeuAc, *N*-acetylneuraminic acid; NeuGc, *N*-glycolylneuraminic acid; PNGase F, peptide *N*-glycosidase F; sICAM-1, soluble intercellular adhesion molecule-1; TFA, trifluoroacetic acid.

References

Angata, T., Kerr, S.C., Greaves, D.R., Varki, N.M., Crocker, P.R., and Varki, A. (2002) Cloning and characterization of human Siglec-11. A recently evolved signaling that can interact with SHP-1 and SHP-2 and is expressed by tissue macrophages, including brain microglia. *J. Biol. Chem.*, **277**, 24466–24474.

Bloom, J.W., Madanat, M.S., and Ray, M.K. (1996) Cell line and site specific comparative analysis of the N-linked oligosaccharides on human ICAM-1des454–532 by electrospray ionization mass spectrometry. *Biochemistry*, **35**, 1856–1864.

Budnik, A., Grewe, M., Gyufko, K., and Krutmann, J. (1996) Analysis of the production of soluble ICAM-1 molecules by human cells. *Exp. Hematol.*, **24**, 352–359.

Chen, W. and Stanley, P. (2003) Five Lec1 CHO cell mutants have distinct Mgat1 gene mutations that encode truncated N-acetylglucosaminyltransferase I. *Glycobiology*, **13**, 43–50.

Chenu, S., Gregoire, A., Malykh, Y., Visvikis, A., Monaco, L., Shaw, L., Schauer, R., Marc, A., and Goergen, J.L. (2003) Reduction of CMP-N-acetylneuraminic acid hydroxylase activity in engineered Chinese hamster ovary cells using an antisense-RNA strategy. *Biochim. Biophys. Acta*, **1622**, 133–144.

Coddeville, B., Regoeczi, E., Strecker, G., Plancke, Y., and Spik, G. (2000) Structural analysis of trisialylated biantennary glycans isolated from mouse serum transferrin. Characterization of the sequence Neu5Gc(alpha 2–3)Gal(beta 1–3)[Neu5Gc(alpha 2–6)]GlcNAc(beta 1–2)Man. *Biochim. Biophys. Acta*, **1475**, 321–328.

Dell, A. and Morris, H.R. (2001) Glycoprotein structure determination by mass spectrometry. *Science*, **291**, 2351–2356.

Delmotte, P., Degroote, S., Lafitte, J.J., Lamblin, G., Perini, J.M., and Roussel, P. (2002) Tumor necrosis factor alpha increases the expression of glycosyltransferases and sulfotransferases responsible for the biosynthesis of sialylated and/or sulfated Lewis x epitopes in the human bronchial mucosa. *J. Biol. Chem.*, **277**, 424–431.

Diamond, M.S., Staunton, D.E., de Fougerolles, A.R., Stacker, S.A., Garcia-Aguilar, J., Hibbs, M.L., and Springer, T.A. (1990) ICAM-1 (CD54): a counter-receptor for Mac-1 (CD11b/CD18). *J. Cell Biol.*, **111**, 3129–3139.

Diamond, M.S., Staunton, D.E., Marlin, S.D., and Springer, T.A. (1991) Binding of the integrin Mac-1 (CD11b/CD18) to the third immunoglobulin-like domain of ICAM-1 (CD54) and its regulation by glycosylation. *Cell*, **65**, 961–971.

Dustin, M.L., Rothlein, R., Bhan, A.K., Dinarello, C.A., and Springer, T.A. (1986) Induction by IL, 1 and interferon-gamma: tissue distribution, biochemistry, and function of a natural adherence molecule (ICAM-1). *J. Immunol.*, **137**, 245–254.

Garcia-Vallejo, J.J., van Dijk, W., van Die, I., and Gringhuis, S.I. (2005) Tumor necrosis factor-alpha up-regulates the expression of beta1,4-galactosyltransferase I in primary human endothelial cells by mRNA stabilization. *J. Biol. Chem.*, **280**, 12676–12682.

Greenwood, J., Etienne-Manneville, S., Adamson, P., and Couraud, P.O. (2002) Lymphocyte migration into the central nervous system: Implication of ICAM-1 signalling at the blood–brain barrier. *Vasc. Pharmacol.*, **38**, 315–322.

Jimenez, D., Roda-Navarro, P., Springer, T.A., and Casasnovas, J.M. (2005) Contribution of N-linked glycans to the conformation and function of intercellular adhesion molecules (ICAMs). *J. Biol. Chem.*, **280**, 5854–5861.

King, P.D., Sandberg, E.T., Selvakumar, A., Fang, P., Beaudet, A.L., and Dupont, B. (1995) Novel isoforms of murine intercellular adhesion molecule-1 generated by alternative RNA splicing. *J. Immunol.*, **154**, 6080–6093.

Klickstein, L.B., York, M.R., Fougerolles, A.R., and Springer, T.A. (1996) Localization of the binding site on intercellular adhesion molecule-3 (ICAM-3) for lymphocyte function-associated antigen, 1 (LFA-1). *J. Biol. Chem.,* **271**, 23920–23927.

Kuster, B. and Mann, M. (1999), ^{18}O-labeling of N-glycosylation sites to improve the identification of gel-separated glycoproteins using peptide mass mapping and database searching. *Anal. Chem.,* **71**, 1431–1440.

Kusterer, K., Bojunga, J., Enghofer, M., Heidenthal, E., Usadel, K.H., Kolb, H., and Martin, S. (1998) Soluble ICAM-1 reduces leukocyte adhesion to vascular endothelium in ischemia-reperfusion injury in mice. *Am. J. Physiol.*, **275**, G377–G380.

Lee, K., Jin, X., Zhang, K., Copertino, L., Andrews, L., Baker-Malcolm, J., Geagan, L., Qiu, H., Seiger, K., Barngrover, D., McPherson, J.M., and Edmunds, T. (2003) A biochemical and pharmacological comparison of enzyme replacement therapies for the glycolipid storage disorder Fabry disease. *Glycobiology*, **13**, 305–313.

Lyons, P.D. and Benveniste, E.N. (1998) Cleavage of membrane-associated ICAM-1 from astrocytes: involvement of a met alloprotease. *Glia*, **22**, 103–112.

Marlin, S.D. and Springer, T.A. (1987) Purified intercellular adhesion molecule-1 (ICAM-1) is a ligand for lymphocyte function-associated antigen, 1 (LFA-1). *Cell*, **51**, 813–819.

McCabe, S.M., Riddle, L., Nakamura, G.R., Prashad, H., Mehta, A., Berman, P.W., and Jardieu, P. (1993) sICAM-1 enhances cytokine production stimulated by alloantigen. *Cell. Immunol.*, **150**, 364–375.

Meyer, D.M., Dustin, M.L., and Carron, C.P. (1995) Characterization of intercellular adhesion molecule-1 ectodomain (sICAM-1) as an inhibitor of lymphocyte function-associated molecule–1 interaction with ICAM-1. *J. Immunol.*, **155**, 3578–3584.

Millan, J. and Ridley, A.J. (2005) Rho GTPases and leucocyte-induced endothelial remodelling. *Biochem. J.*, **385**, 329–337.

Muhlenhoff, M., Manegold, A., Windfuhr, M., Gotza, B., and Gerardy-Schahn, R. (2001) The impact of N-glycosylation on the functions of polysialyltransferases. *J. Biol. Chem.*, **276**, 34066–34073.

Nadanaka, S., Sato, C., Kitajima, K., Katagiri, K., Irie, S., and Yamagata, T. (2001) Occurrence of oligosialic acids on integrin alpha, 5 subunit and their involvement in cell adhesion to fibronectin. *J. Biol. Chem.*, **276**, 33657–33664.

Otto, V.I., Gloor, S.M., Frentzel, S., Gilli, U., Ammann, E., Hein, A.E., Folkers, G., Trentz, O., Kossmann, T., and Morganti-Kossmann, M.C. (2002) The production of macrophage inflammatory protein-2 induced by soluble intercellular adhesion molecule-1 in mouse astrocytes is mediated by src tyrosine kinases and p42/44 mitogen-activated protein kinase. *J. Neurochem.*, **80**, 824–834.

Otto, V.I., Heinzel-Pleines, U.E., Gloor, S.M., Trentz, O., Kossmann, T., and Morganti-Kossmann, M.C. (2000) sICAM-1 and TNF-alpha induce MIP-2 with distinct kinetics in astrocytes and brain microvascular endothelial cells. *J. Neurosci. Res.*, **60**, 733–742.

Otto, V.I., Schurpf, T., Folkers, G., and Cummings, R.D. (2004) Sialylated complex-type N-glycans enhance the signaling activity of soluble intercellular adhesion molecule-1 in mouse astrocytes. *J. Biol. Chem.*, **279**, 35201–35209.

Packer, N.H., Lawson, M.A., Jardine, D.R., and Redmond, J.W. (1998) A general approach to desalting oligosaccharides released from glycoproteins. *Glycoconj. J.*, **15**, 737–747.

Petrescu, A.J., Milac, A.L., Petrescu, S.M., Dwek, R.A., and Wormald, M.R. (2004) Statistical analysis of the protein environment of N-glycosylation sites: implications for occupancy, structure, and folding. *Glycobiology*, **14**, 103–114.

Rancan, M., Otto, V.I., Hans, V.H., Gerlach, I., Jork, R., Trentz, O., Kossmann, T., and Morganti-Kossmann, M.C. (2001) Upregulation of ICAM-1 and MCP-1 but not of MIP-2 and sensorimotor deficit in response to traumatic axonal injury in rats. *J. Neurosci. Res.*, **63**, 438–446.

Rieckmann, P., Michel, U., Albrecht, M., Bruck, W., Wockel, L., and Felgenhauer, K. (1995) Soluble forms of intercellular adhesion molecule-1 (ICAM-1) block lymphocyte attachment to cerebral endothelial cells. *J. Neuroimmunol.*, **60**, 9–15.

Sato, C., Fukuoka, H., Ohta, K., Matsuda, T., Koshino, R., Kobayashi, K., Troy, F.A., 2nd, and Kitajima, K. (2000) Frequent occurrence of pre-existing alpha 2→8-linked disialic and oligosialic acids with chain lengths up to 7 Sia residues in mammalian brain glycoproteins. Prevalence revealed by highly sensitive chemical methods and anti-di-, oligo-, and poly-Sia antibodies specific for defined chain lengths. *J. Biol. Chem.,* **275**, 15422–15431.

Sato, C., Matsuda, T., and Kitajima, K. (2002) Neuronal differentiation-dependent expression of the disialic acid epitope on CD166 and its involvement in neurite formation in Neuro2A cells. *J. Biol. Chem.*, **277**, 45299–45305.

Shevchenko, A., Wilm, M., Vorm, O., and Mann, M. (1996) Mass spectrometric sequencing of proteins silver-stained polyacrylamide gels. *Anal. Chem.*, **68**, 850–858.

Sobel, R.A., Mitchell, M.E., and Fondren, G. (1990) Intercellular adhesion molecule-1 (ICAM-1) in cellular immune reactions in the human central nervous system. *Am. J. Pathol.*, **136**, 1309–1316.

Stanley, P. and Chaney, W. (1985) Control of carbohydrate processing: the lec1A CHO mutation results in partial loss of N-acetylglucosaminyltransferase I activity. *Mol. Cell. Biol.*, **5**, 1204–1211.

Townsend, R.R., Lipniunas, P.H., Bigge, C., Ventom, A., and Parekh, R. (1996) Multimode high-performance liquid chromatography of fluorescently labeled oligosaccharides from glycoproteins. *Anal. Biochem.*, **239**, 200–207.

Varki, A., Cummings, R.D., Esko, J., Freeze, H., Hart, G., and Marth, J. (1999) *Essentials of Glycobiology*. Cold Spring Harbor Laboratory Press, Cold Spring Harbor, New York.

Viseux, N., Hronowski, X., Delaney, J., and Domon, B. (2001) Qualitative and quantitative analysis of the glycosylation pattern of recombinant proteins. *Anal. Chem.*, **73**, 4755–4762.

Yang, Y., Jun, C.D., Liu, J.H., Zhang, R., Joachimiak, A., Springer, T.A., and Wang, J.H. (2004) Structural basis for dimerization of ICAM-1 on the cell surface. *Mol. Cell*, **14**, 269–276.

Yasukawa, Z., Sato, C., and Kitajima, K. (2005) Inflammation-dependent changes in alpha2,3-, alpha2,6-, and alpha2,8-sialic acid glycotopes on serum glycoproteins in mice. *Glycobiology*, 15, 827–837.

Yasukawa, Z., Sato, C., Sano, K., Ogawa, H., and Kitajima, K. (2006) Identification of disialic acid-containing glycoproteins in mouse serum: a novel modification of immunoglobulin light chains, vitronectin, and plasminogen. *Glycobiology*, **16**, 651–665.

Zhang, J.Q., Biedermann, B., Nitschke, L., and Crocker, P.R. (2004) The murine inhibitory receptor mSiglec-E is expressed broadly on cells of the innate immune system whereas mSiglec-F is restricted to eosinophils. *Eur. J. Immunol.*, **34**, 1175–1184.